

## Asymmetric growth in micelles containing oil

Peter H. Nelson,<sup>a)</sup> T. Alan Hatton, and Gregory C. Rutledge<sup>b)</sup>

*Department of Chemical Engineering, Massachusetts Institute of Technology, Cambridge, Massachusetts 02139*

(Received 14 December 1998; accepted 22 February 1999)

The effect of oil on the equilibrium microstructure of a dilute micellar solution is investigated using lattice Monte Carlo techniques. Dramatic growth of the self-assembled micelles into elongated worms is observed as oil is solubilized within the oily tail region of the micelles. These results confirm a microscopic explanation for experimentally observed changes in the phase behavior of surfactant solutions as oil is added. In these simulations, a two-box simulation technique is used to guarantee that the micellar system is stable with respect to emulsification failure (the appearance of a bulk oil phase). © 1999 American Institute of Physics. [S0021-9606(99)70219-9]

### I. INTRODUCTION

Dilute solutions of surfactants are commonly used to solubilize hydrophobic compounds in aqueous solution. A familiar example is dishwashing, where household detergents (surfactants) are used to dissolve oil and grease in water. The ability of surface-active agents to solubilize hydrophobic molecules is central to understanding an extremely wide range of natural systems from subcellular biological to transcontinental geological systems.<sup>1</sup> Industrial applications range from enhanced oil recovery and cleanup of ground water contaminated with hydrophobic pollutants, to stabilizing cosmetics and foodstuffs. Medical applications range from drug delivery to providing understanding of basic biological processes.

Recently, molecular dynamics simulations<sup>2-4</sup> and experiments<sup>5-7</sup> have been conducted to investigate the dynamics of the initial oil solubilization process by surfactant solutions. In the nonequilibrium simulations of Karaborni *et al.*,<sup>2</sup> three mechanisms were identified for transport of oil molecules from an oil droplet to the hydrophobic cores of the micelles; (1) desorption of oil molecules from the oil droplet into the aqueous phase followed by capture in a micelle; (2) exchange of oil molecules between the oil droplet and micelles during a soft collision; and (3) collective desorption of oil molecules from the oil droplet surface. As these simulations<sup>2-4</sup> were far from equilibrium, the effect of the solubilized oil on equilibrium micellar structure was not investigated.

Extensive equilibrium studies of oil-water-surfactant systems have been conducted by Larson in recent years<sup>8-12</sup> using a lattice model. The rich phase behavior of (mainly) ordered condensed phases of systems with high (>20%) surfactant concentrations was successfully demonstrated using this model. The structure and properties of disordered systems with low oil and surfactant concentrations have gone largely unexplored. In this paper, a lattice model similar to

that of Larson<sup>8-12</sup> is used to investigate the effect of small amounts of oil on the equilibrium microstructure of dilute (7.5% by volume) surfactant solutions. A two-box simulation technique is used to guarantee that the equilibrium microemulsion is stable with respect to emulsification failure (appearance of a bulk oil phase), and the partition coefficient between the micellar solution and a bulk aqueous phase is measured directly.

### II. SIMULATION METHOD

As described in Ref. 13, the main simulation box (the micelle box) is a face centered cubic (fcc) lattice with the usual periodic boundary conditions applied. The lattice contains a symmetric H<sub>2</sub>T<sub>2</sub> surfactant, which has two “hydrophilic” head beads (H) and two “hydrophobic” tail beads (T). Single-bead “oil” molecules (O) are also present and the remainder of the lattice is filled with water beads (W). The oil molecules interact with the other beads as if they were hydrophobic tail beads. The hydrophilic/hydrophobic nearest neighbor interactions are set to  $\epsilon$  and all other interactions are set to zero as has been done previously.<sup>13-16</sup> This makes the oil a good (athermal) solvent for the tail blocks of the surfactant (e.g., hexane and a C<sub>12</sub> surfactant tail) and the water a good solvent for the head beads. The general reptation method developed previously<sup>13,16</sup> is used to make configurational changes in the simulation and a combination of the bead and vacancy algorithms is used to move the oil and surfactant molecules through the lattice.

In addition to the micelle box, a water box is set up that is of the same size as the micelle box (with periodic boundary conditions) but contains no surfactant. The oil beads in the water box are made to move by exchanging places with neighboring water beads. Oil beads, in both the micelle box and the water box, are also selected randomly for exchange with a water bead in a randomly selected lattice site in the other simulation box. Boltzmann weighting factors are calculated for the initial and final states of all trial moves so that the Metropolis sampling technique<sup>17</sup> can be applied, and the chemical potentials of the oil and the water are the same in both boxes. Although the two simulation boxes are not in

<sup>a)</sup>Present address: Department of Chemistry, University of Massachusetts, Amherst Massachusetts 01003.

<sup>b)</sup>Author to whom correspondence should be addressed.

physical contact, this arrangement is thermodynamically equivalent to having them in contact but separated by a rigid diathermal semipermeable membrane that allows water and oil to pass but is impermeable to the surfactant. In general, there will be an osmotic pressure difference between the two boxes.

Two-box simulations for studying phase equilibria under various conditions have been explored in some detail by Pangiopoulos and co-workers.<sup>18–20</sup> The approach taken in this work is to eliminate volume moves from the simulation scheme so that each of the boxes has fixed volume,<sup>13</sup> similar to the membrane equilibrium approach described by Pangiopoulos *et al.*,<sup>20</sup> but with two permeating components (oil and water) and a spontaneous osmotic pressure set up by the nonpermeating surfactant.

The simulation method used here can be easily applied to molecules larger than a single lattice site if there is a monomeric solvent (or voids) present in the lattice. For example, we could double the molecular weight of our oil molecule to be two connected oil beads. The constant volume exchange between the water box and the micelle box can be achieved by selecting an oil molecule at random from either of the two boxes and two adjacent lattice sites in the other box and the simulation method can proceed as before.

An alternative approach that has been used in similar surfactant systems<sup>12</sup> employs a single simulation box in the grand-canonical ensemble. In that approach, oil beads replace water beads and vice versa using a Boltzmann weight that has the specified chemical potential difference between oil and water  $\Delta\mu$  added to it. The requirement that  $\Delta\mu$  must be specified as an input to the simulation is an additional complication compared with the two-box method used here. In addition, this open system method does not work as well for chemical potential differences close to that between bulk water and oil phases. Under these conditions, the single-box system is able to fluctuate between the mostly water phase on one side of the phase diagram and the mostly oil phase on the other side of the phase diagram causing further procedural difficulties in measuring equilibrium properties. Oil/water concentration fluctuations in the two-box simulation are limited by the constraint that the amount of oil/water in the combined system is constant throughout a simulation. This has the advantage that we can approach the phase boundary more closely without oscillating between the two phases that can coexist across a tie line on the phase diagram. With the two-box method used here, it is also possible to move past the coexistence line into a supersaturated region of the phase diagram, where the concentration of the oil in the water box is higher than its equilibrium solubility and the properties of metastable emulsions can, in principle, be investigated. Thus, in this work, we are able to closely approach the phase boundary for emulsification failure. Simulations of metastable emulsions were also conducted in this study but the results were significantly affected by finite size effects, see Ref. 13 and the discussion below.

The water box is a simple oil–water system with no surfactant. If the measured concentration of oil in the water box is below the equilibrium oil solubility, then we are assured that the micelle box is a stable microemulsion not sub-

ject to “emulsification failure.” Emulsification failure occurs<sup>1</sup> when all the oil in an emulsion cannot be solubilized in the water phase so that a bulk phase of oil coexists with the microemulsion at equilibrium. In this study, we are interested in determining the partition coefficient of the oil between the micellar system and a bulk water phase. The two-box simulation method used here is ideally suited for investigating the partitioning across a rigid semipermeable membrane as the concentration in each phase can be measured directly.

### III. SIMULATION RESULTS

#### A. Equilibrium oil solubility

The free energy of mixing for a dilute solution of oil in water with concentration  $x$  on a lattice can be written as

$$\frac{\Delta G_{\text{mix}}}{k_B T} = \chi x(1-x) + x \ln(x) + (1-x) \ln(1-x)$$

using the mean-field approximation for the enthalpy of mixing and the ideal solution expression for the entropy of mixing;  $k_B$  is the Boltzmann constant,  $T$  is the temperature, and  $\chi = z\epsilon/k_B T$  is the Flory–Huggins  $\chi$ -parameter for our lattice system with coordination number  $z$  and interaction strength  $\epsilon$ . For all the simulations reported here,  $\chi = 6$ , and the free energy has a minimum at  $x = 0.00255$ , which is the equilibrium solubility of the oil in water. The mean-field and ideal entropy of mixing approximations are justified *a posteriori* by the low value of  $x$  obtained (both these approximations become very good at low concentrations).

The two-box simulation method used here can easily be applied to this binary system of oil and water beads. The phase equilibrium between the two bulk phases was investigated by filling one box with oil beads (the oil box) and filling the other box (the water box) with pure water. The simulation proceeded as described above with the simplification that there was no surfactant in the oil (micelle) box. The equilibrium oil concentration (solubility) of the oil in water was determined and a value of  $x = 0.00254 \pm 0.0001$  was obtained (cf. theoretical prediction of  $x = 0.00255$ ), confirming that the two-box simulation method correctly reproduces bulk oil/water phase equilibria.

#### B. Equilibration

All the simulations reported in this paper were conducted using a surfactant volume fraction of 7.5% as used in Ref. 15 for a surfactant–water only system. The amount of oil in the combined two-box system was the only independent variable. A preliminary simulation run was conducted on a  $40 \times 40 \times 40$  fcc lattice with 9600 oil molecules (15% of the volume of the micelle box) and 1200 surfactant molecules (7.5% of the volume of the micelle box). This system was equilibrated until a single oil droplet formed in the micelle box. The oil content in this system was then adjusted as described below to generate initial configurations with large aggregates. The advantage of starting with large aggregates is that their stability can be determined for various solution conditions without having to wait for them to form spontaneously.

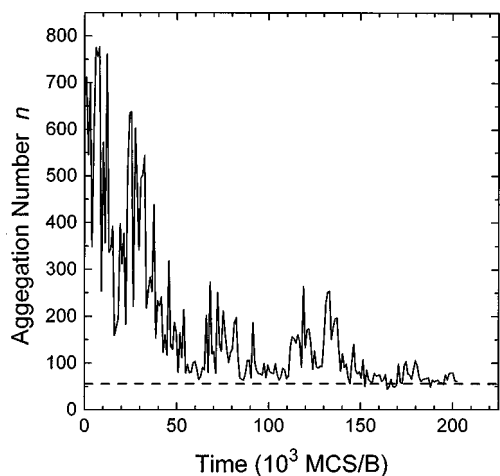


FIG. 1. Approach to equilibrium of the micellar aggregation state of a two-box simulation with an oil/surfactant molecular ratio of 1/10. The dashed line indicates the equilibrium value (see text).

The amount of oil in the micelle box was reduced by performing preliminary simulation runs, in which oil transferred to the water box was not allowed to return to the micelle box. Once the desired oil concentration in the micelle box was reached, the surplus oil beads, now located in the water box, were removed from the simulation and replaced with water beads. Equilibration then proceeded with the oil particles being allowed to exchange freely between the two simulation boxes in the normal way. During equilibration, the instantaneous average aggregation number of the system was monitored to gauge when equilibrium was reached. As discussed in Refs. 13 and 15, the time development of the average aggregation number of the system is significantly more sensitive to deviations from equilibrium than the configurational energy.

Figure 1 shows how the aggregation state of a system with 120 oil molecules develops with time. The initial large aggregates break up spontaneously into smaller micelles that diffuse apart and spread out randomly throughout the micelle box until the equilibrium value of 55.8 (dashed line) is reached at about  $2 \times 10^5$  Monte Carlo steps per (oil or surfactant) bead (MCS/B). The main simulation was started using the ultimate configuration of the equilibration simulation and was run for much longer ( $10^7$  MCS/B), to collect the equilibrium data (such as the dashed line).

The large downward jumps in Fig. 1 are caused by micelles breaking up into smaller micelles and the large upward jumps correspond to the coalescence of micelles. As the system approaches equilibrium, these two processes reach a kinetic balance and the aggregate size distribution approaches equilibrium. At equilibrium, in this system, mechanisms (2) and (3) identified by Karaborni *et al.*<sup>2</sup> become equivalent and there are just two mechanisms for oil transport between aggregates, “desorption followed by capture” and “micellar coalescence/breakup.” In the first mechanism, an oil molecule desorbs from a micelle and diffuses through the aqueous phase to another micelle where it is captured in its hydrophobic tail region. This mechanism is most important for small oil molecules, such as those used here, whose solubil-

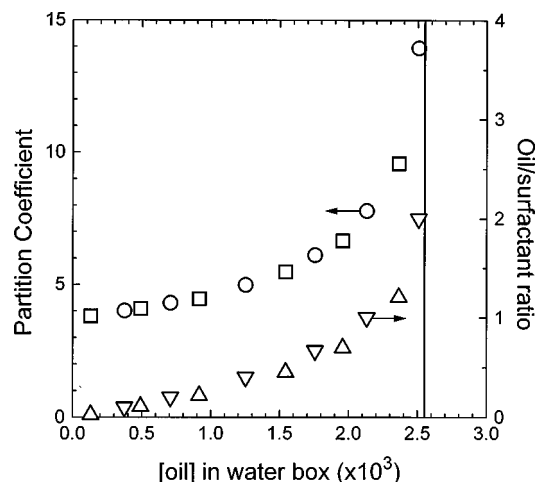


FIG. 2. Partition coefficient of oil between a micellar phase containing 7.5% surfactant by volume and a bulk water phase, as a function of oil concentration in the water phase. Circles are from a larger system ( $40 \times 40 \times 40$ ) and squares are from a smaller system ( $20 \times 20 \times 20$ ). Also shown are the total oil/surfactant molecular ratios in the two-box simulation, which can be used as a key to go between discussions where we use the oil concentration in the water box to characterize the system and those where we use the total oil/surfactant ratio. The vertical line indicates the phase boundary for emulsification failure.

ity in (pure) water is not vanishingly small. The second mechanism occurs when two micelles coalesce or a micelle breaks in two. During a collision the hydrophobic regions of the two micelles touch and oil molecules can be exchanged between them without the oil having to desorb into the water. Micellar breakup occurs with equal probability as coalescence at equilibrium. If the two micelles break apart after a short time after coalescence then the soft collision mechanism (2) identified by Karaborni *et al.*<sup>2</sup> has occurred.

### C. Oil partitioning across a semipermeable membrane

The ability of surfactant solutions to dissolve more oil than aqueous solutions can be quantified by a partition coefficient,

$$K = \frac{c_m}{c_w},$$

where  $c_m$  is the concentration of oil in the micelle box and  $c_w$  is the concentration of oil in the water box. This partition coefficient is slightly different from the one often used to quantify partitioning between the micelles themselves and the surrounding fluid. The partition coefficient is shown in Fig. 2 as a function of oil concentration for the systems investigated. Small system ( $20 \times 20 \times 20$ ) values are shown as squares and large system ( $40 \times 40 \times 40$ ) values are shown as circles. Also shown is the total oil/surfactant ratio in the two-box simulation, which can be used as a key to go between discussions where we use the oil concentration in the water box to characterize the system and those where we use the total oil/surfactant ratio. The highest oil concentration in Fig. 2 has a ratio of two oil molecules per surfactant molecule. This makes the volume fraction of surfactant tails and oil molecules approximately equal in the micelle box.

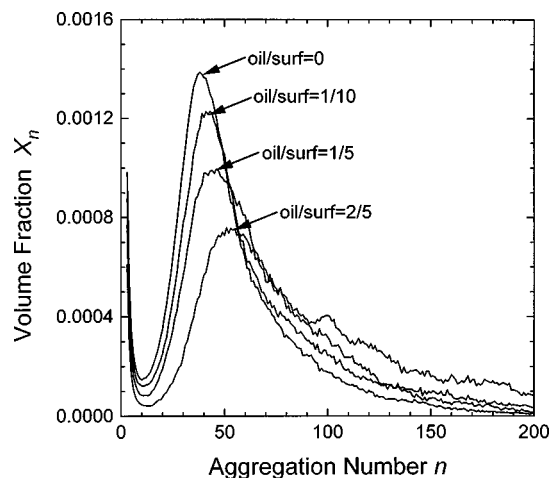


FIG. 3. Changes in the micellar size distribution as small amounts of oil are added. Numerical values indicate the oil/surfactant molecular ratio in the two-box simulation.

The behavior shown in Fig. 2 is comparable to that found experimentally.<sup>21</sup> At low oil concentrations, the partition coefficient increases slowly with  $c_w$ . However, as  $c_w$  approaches the bulk solubility the partition coefficient increases rapidly. The large values of the partition coefficient indicate that the surfactant system is able to solubilize many times more oil than the bulk water phase in the water box. As we show below, most of the oil is contained within the oily region formed by the surfactant tails in the micelles.

Figure 3 shows the size distributions of micellar aggregates obtained from the  $40 \times 40 \times 40$  simulations of dilute oil-water-surfactant systems with small amounts of added oil. The ratios of oil to surfactant in the combined two-box system range from zero to a ratio of 2/5. The results for zero added oil were reported previously.<sup>15</sup> The definition of an aggregate used in Ref. 15 is modified to account for the presence of oil molecules. An aggregate is defined as a collection of oily surfactant tails and oil molecules that are touching each other. It is no longer necessary for all the surfactant tails of an aggregate to touch each other directly, since they may be connected by regions of oil molecules. The aggregation number of an aggregate is still defined as the number of surfactant molecules in the aggregate.

The peak in the distribution shifts to higher aggregation numbers as oil is added. This indicates that the spherical aggregates become larger and the oily core of the micelle is expanded by the absorbed oil, thereby increasing the surface area available for the surfactant molecules. The height of the peak decreases with oil concentration while the width (full-width at half-maximum) increases and there is an increasing proportion of surfactant in the tail portion of the distribution ( $n \geq 100$ ) as the amount of added oil increases. This exponential tail contains cylindrical micelles.<sup>13,15</sup> All these changes are consistent with the swelling and growth of micelles upon addition of small amounts of oil.

#### D. Dramatic micellar growth

Above an oil surfactant ratio of 2/5, adding more oil to the system significantly alters the micellar size distribution.<sup>13</sup>

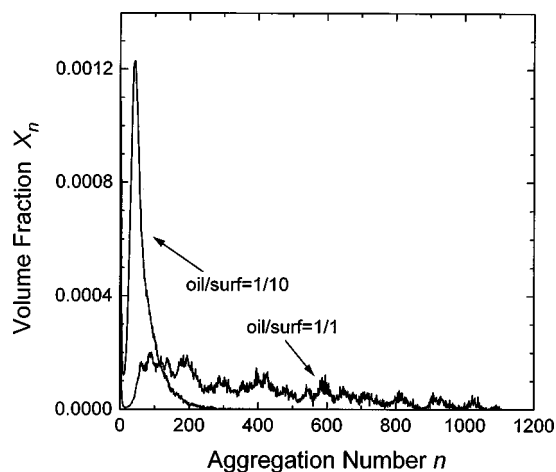


FIG. 4. Comparison of micellar size distributions in two-box simulations with oil/surfactant molecular ratios of 1/10 and 1/1.

Figure 4 shows the data from the simulation with equal numbers of oil and surfactant molecules together with the 1/10 oil/surfactant ratio simulation. The scale of the horizontal axis has been increased sixfold relative to Fig. 3 to show the long tail of the 1/1 distribution, which has an average aggregation number of about 300. There is a large amount of scatter in the distribution, so that the true shape of the size distribution cannot be determined precisely. This scatter is caused primarily by the considerable width of the distribution. As we have seen previously,<sup>13,15</sup> the time required to obtain a smooth distribution can be estimated as

$$\tau_{\text{dist}} \sim \frac{\langle a \rangle \langle a^2 \rangle \tau_{aa}}{N_s},$$

where  $\langle a \rangle$  is the average aggregation number,  $\langle a^2 \rangle$  is the mean-square aggregation number,  $\tau_{aa}$  is the characteristic time for desorption of a monomer from a micelle, and  $N_s$  is the number of surfactant molecules in the simulation.

If we compare the simulations with oil/surfactant ratios of 1/10 and 1/1 (see Fig. 4), we observe that  $N_s$  is the same for both,  $\tau_{aa}$  has similar values, but  $\langle a \rangle$  is over five times larger and  $\langle a^2 \rangle$  is over 30 times larger. Hence, we can estimate that the higher oil concentration simulation will need to execute for more than 150 times longer to obtain the same smoothness in the size distribution as the lower oil concentration simulation. The data in Fig. 4 were generated from  $5 \times 10^{10}$  Monte Carlo steps (or  $8.3 \times 10^6$  MCS/B for the oil/surfactant = 1/1 simulation) and took 13 days of execution time on an IBM RS/6000 model 370. Hence, we estimate that a smooth distribution would require 5 years to be produced using the same machine.

The shapes of the aggregates of different sizes can be determined from the principal moments of the radius of gyration tensor (see Refs. 13 and 15). The oil beads are included in the determination of the average shape of the aggregates. Figure 5 shows the shape distribution obtained from the simulation with an oil/surfactant ratio of 1/1. True micelles begin to form at an aggregation number of about 50 and the three components of the radius of gyration tensor are approximately equal, indicating that these small aggregates

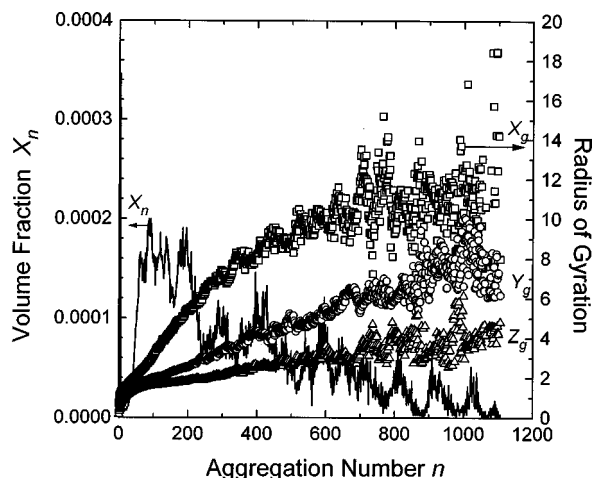


FIG. 5. Micellar shape distributions in a two-box simulation with an oil/surfactant molecular ratio of 1/1.  $X_g$ ,  $Y_g$  and  $Z_g$  are the ordered principle components of the radius of gyration tensor.

are roughly spherical. The instantaneous shapes of the micelles are not perfectly spherical and the principle components are ordered before averaging, so even small fluctuations in shape are sufficient to account for the differences between the three values in Fig. 5 at an aggregation number of about 50.

In the size range from 50 to 300, the micelles begin to grow in one direction to form spherically capped cylinders, with approximately the same minimum dimension as the 50-spheres. For comparison, note that for a cylinder of length  $2L$  and radius  $R$ ,  $Y_g$ , and  $Z_g$  are equal to each other and are proportional to  $R$ , while  $X_g$  is proportional to  $L$ . As the micelles grow longer, the cylinders become more flexible and  $X_g$  falls below the linear form expected for rigid cylinders. This flexibility also explains why  $Y_g$  and  $Z_g$  increase from the constant value expected for rigid cylinders as the micelles become more wormlike. These observations were also confirmed by visualization and inspection of snapshots of the system (e.g., see Fig. 6). As the size of the micelles increases further, they become more threadlike and may contain one or more branch points. The largest aggregate in Fig. 6(b) contains 429 surfactant molecules and has a well-defined branch point.

The size distributions of the micelles containing oil are qualitatively similar to the distributions observed in surfactant-only micelles,<sup>13,15</sup> having a peak of spherical micelles in equilibrium with an exponential tail of cylindrical micelles. In the surfactant only systems, the aggregation number of the spherical peak remains approximately constant as the micelles grow upon addition of more surfactant, whereas in the present study the spherical peak shifts to higher aggregation numbers as oil is added to the micelles, indicating that the spherical micelles are swollen as oil is absorbed into them. Another difference is that adding oil to a 7.5% surfactant solution produces greater micellar growth than adding an equal concentration of surfactant molecules. For example, the average aggregation number of the 1/1 oil/surfactant system is more than three times that of the 15%

surfactant-only solution in Ref. 15, and the mean-square aggregation number is more than ten times larger.

### E. Oil location in micelles

It has long been recognized that oil molecules mix with the tails of surfactant monolayers.<sup>22</sup> More recently, Aveyard *et al.*<sup>23</sup> proposed a phenomenological model of oil solubilization in surfactant monolayers based on indirect experimental evidence. The model is based on ideas of Mitchell and Ninham,<sup>24</sup> in which *effective* cross-sectional areas  $a_H$  and  $a_T$  are assigned to the head and tail of the surfactant, respectively. The curvature of the surfactant layer may then be related to a packing factor, defined as

$$P = \frac{a_T}{a_H}.$$

The cross-sectional areas, and the packing factor  $P$ , can be affected by the local environment of the head and tail groups. Hence,  $P$  is not determined solely by molecular structure of the surfactant. (If this were the case,  $P$  would be exactly one for our symmetric  $H_2T_2$  surfactant.)

As an example, consider our symmetric surfactant adsorbed at a planar interface between oil and water. The surfactant is symmetric and the solution conditions for the head and tail are equivalent (good solvent conditions), so the packing factor will be unity. However, for a surfactant located in a surfactant-only micelle, the heads are in a good solvent but the tails are in a concentrated solution (or melt) of themselves (with higher concentration). Hence, the tails have an effective cross-sectional area that is lower than that of the heads and the packing factor is less than 1, indicating that the surfactant prefers a positive curvature. As oil is added to the tail region, the concentration of the tail beads is gradually reduced, and the effective cross-sectional area increases until complete saturation occurs and a planar interface is preferred.

These ideas were used by Aveyard *et al.*<sup>23</sup> to provide a molecular level interpretation of the change in cloud point of dilute solutions of the nonionic surfactant  $C_{12}H_{25}(OCH_2CH_2)_6OH$  (commonly referred to as  $C_{12}E_6$ ) upon addition of the oil nonane. The concentration of the  $C_{12}E_6$  surfactant was held constant throughout the experiments, as it is in our simulations. As oil is added to the surfactant solution, the cloud point drops sharply until a minimum is reached at a relatively low oil/surfactant ratio. The cloud point then increases and levels off as saturation is approached.

The molecular level explanation proposed by Aveyard *et al.*<sup>23</sup> for this behavior is as follows. The oil is initially solubilized in the tail regions of the micelles, increasing the value of  $P$  towards unity. The micelles then become more asymmetrical (cylindrical) to reduce the overall surface curvature. This results in increased intermicellar attractions that reduce the cloud point of the solution. As more oil is added, the micelles begin to form a central pool of oil and the aggregates are transformed into spherical microemulsion droplets with an accompanying reduction in intermicellar attractions and hence an increase in the cloud point. However, no

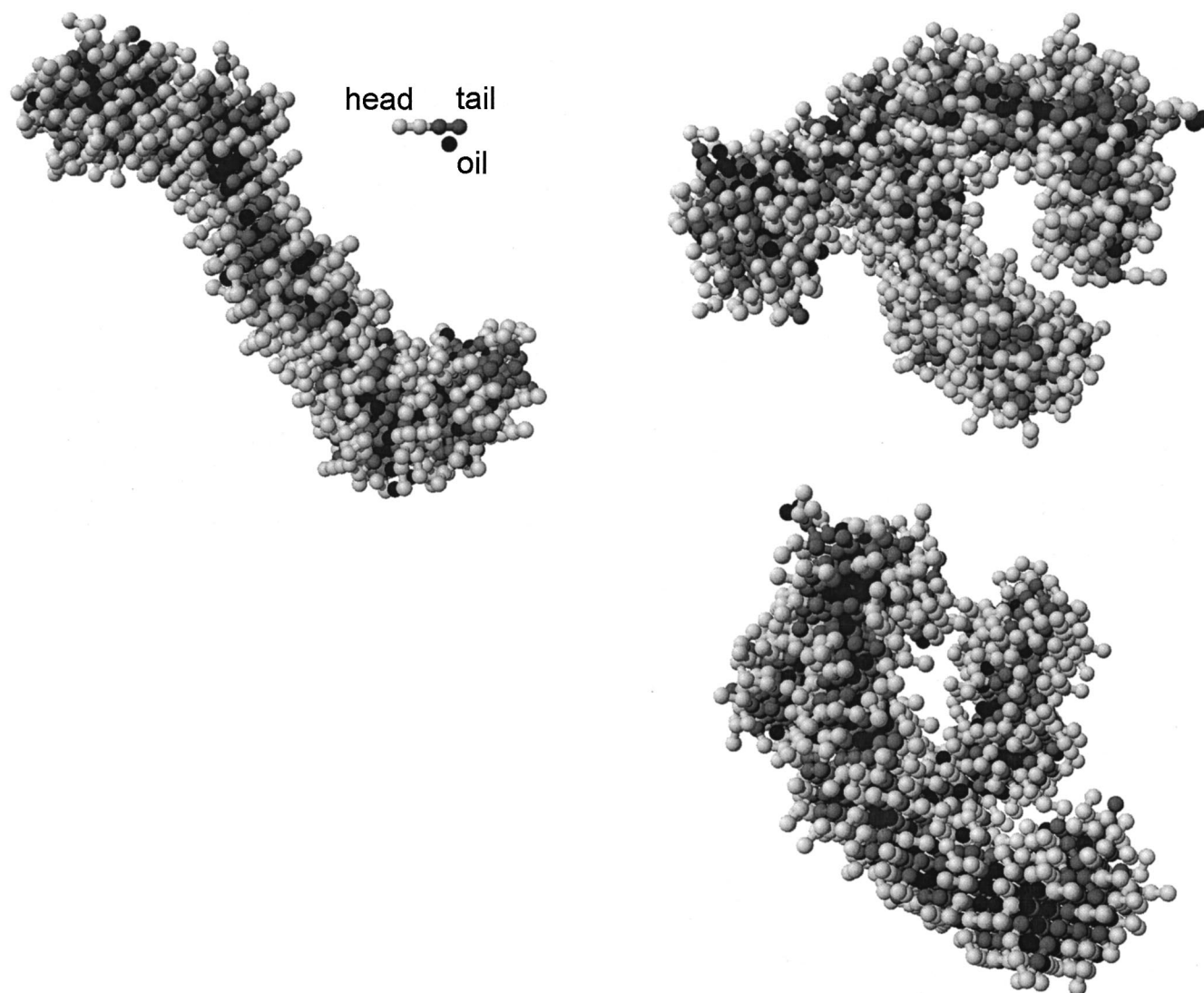


FIG. 6. (a) Snapshot of a micellar aggregate ( $n=288$ ) taken from the final configuration of the two-box simulation with an oil/surfactant molecular ratio of 1/1. Also shown are single surfactant and oil molecules. The darkest beads are oil, the lightest are surfactant head beads, and the intermediate shade represents surfactant tail beads; (b) two views of a branched micellar aggregate ( $n=429$ ) also taken from the final configuration of the two-box simulation with an oil/surfactant molecular ratio of 1/1.

direct measurements were made of the inferred microstructural changes. Aveyard *et al.*<sup>23</sup> also found that longer alkanes tend only to give an increase in cloud point with concentration, from which they inferred that the mechanism for the decrease in cloud point, local mixing of oil and surfactant tails, is stronger for shorter alkanes. Our model system has no long-range attractive forces between the micelles. Hence, the experimental cloud point behavior is unlikely to be directly reproducible in our simulations. However, the microstructural changes, which are believed to be due to local packing effects in the only tail region of the micelles, are demonstrated to occur in our simple model system.

The number of oil molecules in micelles of different sizes is shown in Fig. 7. The amount of oil solubilized in the micelles is directly proportional to the surfactant aggregation number for aggregates larger than about 70. Hence, the oil is absorbed uniformly into the tail regions in micelles of all sizes. This means that the effective cross-sectional area of the tail groups  $a_T$  is increased for all aggregates, which ex-

plains the growth of the cylindrical micelles to reduce interfacial curvature. These simulation results thus provide direct support for the microscopic model of aggregate growth upon oil solubilization proposed by Aveyard *et al.*<sup>23</sup> They also show that the particular chemical details of the solute, solvent and surfactant system studied by Aveyard *et al.* are not necessary for micellar growth; rather, the growth can be caused by simple, universal packing changes in the surfactant tail region of the micelles upon addition of low molecular weight oil that is a good solvent for the tails.

It is also clear from Fig. 7 that the tail region of the micelles is not yet saturated with oil. If the tail regions were saturated, well-defined oil pools would form in the larger aggregates. These spherical aggregates would then have larger oil to surfactant ratios than indicated by the linear fit shown in the figure. Hence, the simulation results lie within the initial downward portion of the cloud point curve of Aveyard *et al.*<sup>23</sup> that was attributed to asymmetric micellar growth. The subsequent development of large spherical ag-

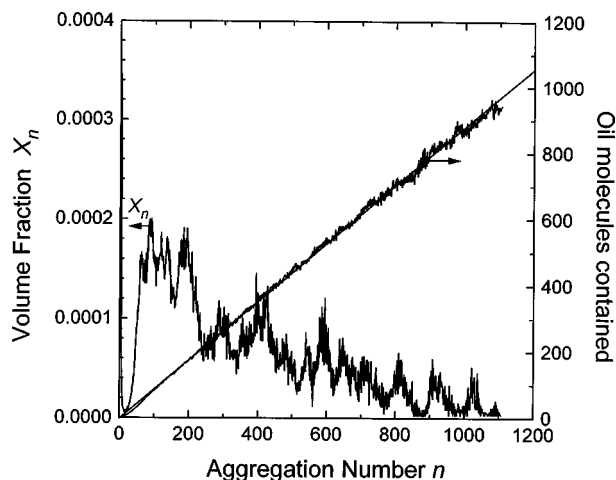


FIG. 7. Distribution of oil molecules in micellar aggregates of different sizes in the two-box simulation with an oil/surfactant molecular ratio of 1/1. The straight line is a least squares fit to the data.

gregates is not observable in our small-scale simulations due to finite size effects.

#### F. Emulsions and finite-size effects

The 1/1 oil/surfactant ratio simulation discussed above is the highest oil concentration simulation that does not appear to be affected significantly by the finite size of the simulation box. (This is not completely certain due to the large statistical uncertainties in its aggregate size distribution shown in Fig. 4.) Finite size effects in the simulation of self-assembling oil–water–surfactant systems are particularly troublesome. The obvious problem is that the largest aggregate that can form is determined by the number of molecules in the box. This can be a significant limitation if many aggregates of large size are expected at equilibrium. A more subtle effect is that the maximum aggregate surface area to volume ratio may be limited by the size of the simulation box (at fixed composition).

As an example of this, consider the preliminary simulation used here to generate initial configurations. The 9600 oil molecule simulation suffers from both these finite size effects. First, the surfactant-coated oil droplet is the largest possible in a 7.5% surfactant, 15% oil system of this size, and hence provides no information on the equilibrium size distribution beyond the trivial fact that aggregates of at least this size are possible. Second, and more significantly, the oil droplet is not representative of any equilibrium microemulsion droplet at the same solution conditions. The small simulation box simply does not contain enough surfactant molecules to coat the outside of a 9600 molecule oil droplet properly. One indication of this is that the oil concentration in the water box (0.00267) is significantly higher than the equilibrium oil solubility (0.00255). This means that the chemical potential of the oil in the droplet is higher than that in a bulk oil phase, indicating that a large system of such droplets would be thermodynamically unstable.

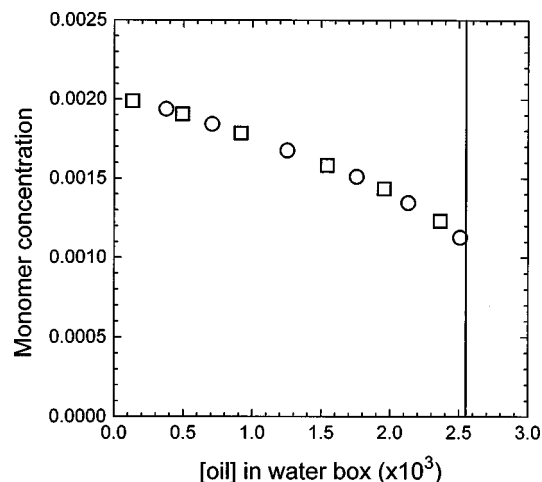


FIG. 8. Surfactant monomer concentration of micellar systems (of constant total surfactant concentration) as a function of oil concentration in the bulk aqueous solution.

#### G. Monomer concentrations (cmc)

It is a commonly made assumption in theories of micellar systems and microemulsions that the concentration of monomers (surfactants with an aggregation number of unity) in the water microphase is constant.<sup>1,25</sup> Figure 8 shows that the monomer concentration of our model decreases significantly as the oil concentration in the water box increases. The decrease in monomer concentration is not due to excluded volume effects, as the volume fraction excluded by the aggregates only changes slightly. The volume fraction of water available for the monomers decreases by less than 5% through the plotted oil concentration range, whereas the monomer concentration decreases by more than 40% through the same range. The large decrease in monomer concentration reflects the change in aggregate geometry with oil concentration. The larger aggregates at higher oil concentrations have lower average curvature due to micellar growth; increasing the length of the cylindrical micelles reduces the fraction of surfactant in the higher curvature spherical end caps. In addition, the minimum dimension of the aggregates increases as more oil is added. Both these effects serve to lower the chemical potential of the surfactant, which prefers low curvature interfaces. This is reflected in the large decrease in the monomer concentration.

An additional contributing factor is that the oil molecules are single beads with no hydrophilic head group attached. This allows the oil beads to move freely throughout the interior and surface of the oily core of the micelle. This serves to increase the packing efficiency of the oily core and help smooth any roughness in the surface. In contrast, longer oil molecules may be less effective in filling small defects in the interior or surface of the oily tail region. This would be consistent with the observation of Aveyard *et al.*<sup>23</sup> that longer alkanes pack less efficiently with the surfactant tails and produce only an increase in cloud point with oil concentration. Finally, the results in Fig. 8 indicate that the critical micellar concentration (cmc) or critical microemulsion concentration ( $c_{\mu c}$ ) of our short surfactant decreases strongly with increasing oil concentration.

Recently, the appropriateness of a single site representation of oil molecules in lattice models of oil–water–surfactant systems was questioned.<sup>12</sup> It was speculated that this representation is such an extreme divergence from reality that even qualitative comparisons could not be made to the phase behavior of real systems when oil is present. The success of the present simulations, in qualitatively reproducing experimentally-inferred microstructural changes of dilute nonionic surfactant solutions as small amounts of low molecular weight oil are added, confirms that the approximation of a single site representation (of low molecular weight oil) is not so extreme as to prevent qualitative comparison with real systems, at least in the present case.

#### IV. CONCLUSION

When oil is added to a surfactant simulation, there is an additional degree of freedom that may allow coexisting phases to appear. To reduce the chance of this occurring, and to measure the oil partition coefficient between the micellar phase and a bulk aqueous solution, a two-box simulation method is used with two constant volume boxes at the same temperature: a micelle box containing oil, water and surfactant; and a water box containing oil and water but no surfactant. In the simulation, oil and water can exchange between the two boxes at constant system volume. This method is equivalent to having the two boxes connected by a rigid diathermal semipermeable membrane so that a spontaneous osmotic pressure difference develops between them.

This method provides a valuable means for probing the chemical potential of oil in micellar systems, equilibrium microemulsions and nonequilibrium emulsion droplets. A simple test for emulsification failure (or the appearance of a bulk oil phase) in the oil-in-water surfactant system is whether the concentration of oil in the water box is above the limit of solubility. As long as this concentration is below the solubility limit, it is guaranteed that the system is stable with respect to emulsification failure. Such guarantees concerning phase behavior are impossible using the traditional single box simulation method in the canonical ensemble.

It is found that small amounts of solubilized oil can have a significant effect on the equilibrium microstructure of a dilute micellar system, producing dramatic one-dimensional growth of the micelles. Asymmetric growth upon addition of oil has previously been proposed by Aveyard *et al.*<sup>23</sup> as an explanation for experimentally observed changes in the macroscopic phase behavior of dilute surfactant solutions as low molecular weight oil was added. The proposal was inferred from cloud point changes and led to a phenomenological description of surfactant behavior based on the “packing factor” (or effective intrinsic curvature). The simulation results therefore provide support not only for the microscopic interpretation of the macroscopic phase behavior, but also the phenomenological concepts upon which the microscopic interpretation was based.

The microscopic picture consistent with experiment and the simulations presented here is that oil added to the solution preferentially absorbs into the oily tail region of the micelles. This reduces the local tail concentration in the oily core of the micelle, and thus increases the effective cross-sectional area of the tails. The packing factor is then increased and the surfactant prefers interfaces with lower overall curvature. Consequently, the micelles grow in one dimension to become the elongated wormlike structures observed in the simulation. This growth is quite dramatic and the average micellar size increases many-fold until the aggregates become branched worm- or thread-like micelles. The simulation results also serve to confirm that the experimentally inferred micellar growth is not necessarily due to the precise chemical nature of the surfactant, oil or solvent, but rather, it can be caused by universal packing changes in the surfactant tail region of the micelles as small oil molecules (that are a good solvent for the surfactant tails) are added to the solution.

- <sup>1</sup>W. M. Gelbart and A. Ben-Shaul, *J. Phys. Chem.* **100**, 13169 (1996).
- <sup>2</sup>S., N. M. Karaborni, K. van Os, P. A. Esselink, and J. Hilbers, *Langmuir* **9**, 1175 (1993).
- <sup>3</sup>S. Karaborni, K. Esselink, P. A. J. Hilbers, B. Smit, J. Karthäuser, N. M. van Os, and R. Zana, *Science* **226**, 254 (1994).
- <sup>4</sup>K. Esselink, P. A. J. Hilbers, N. M. van Os, B. Smit, and S. Karaborni, *Colloids Surf.* **91**, 155 (1994).
- <sup>5</sup>D. J. McClements and S. R. Dungan, *Colloids Surf.* **104**, 127 (1995).
- <sup>6</sup>T. Dam, J. B. F. N. Engberts, J. Karthäuser, S. Karaborni, and N. M. van Os, *Colloids Surf.* **118**, 41 (1996).
- <sup>7</sup>J. Weiss, J. N. Coupland, D. Brathwaite, and D. J. McClements, *Colloids Surf.* **121**, 53 (1997).
- <sup>8</sup>R. G. Larson, *J. Chem. Phys.* **89**, 1642 (1988).
- <sup>9</sup>R. G. Larson, *J. Chem. Phys.* **91**, 2479 (1989).
- <sup>10</sup>R. G. Larson, *J. Chem. Phys.* **96**, 7904 (1992).
- <sup>11</sup>R. G. Larson, *Macromolecules* **27**, 4198 (1994).
- <sup>12</sup>R. G. Larson, *J. Phys. II* **6**, 1441 (1996).
- <sup>13</sup>P. H. Nelson, “Simulation of self-assembled polymer and surfactant systems,” Ph.D. thesis, Massachusetts Institute of Technology, 1998.
- <sup>14</sup>P. H. Nelson, G. C. Rutledge, and T. A. Hatton, *Comput. Theor. Polym. Sci.* **8(1/2)**, 31 (1998).
- <sup>15</sup>P. H. Nelson, G. C. Rutledge, and T. A. Hatton, *J. Chem. Phys.* **107**, 10777 (1997).
- <sup>16</sup>P. H. Nelson, T. A. Hatton, and G. C. Rutledge, *J. Chem. Phys.* **107**, 1269 (1997).
- <sup>17</sup>N. Metropolis, A. W. Rosenbluth, M. N. Rosenbluth, A. H. Teller, and E. Teller, *J. Chem. Phys.* **21**, 1087 (1953).
- <sup>18</sup>A. Z. Panagiotopoulos, *Mol. Phys.* **61**, 813 (1987).
- <sup>19</sup>A. Z. Panagiotopoulos, *Mol. Phys.* **62**, 701 (1987).
- <sup>20</sup>A. Z. Panagiotopoulos, N. Quirke, M. Stapleton, and T. J. Tildesley, *Mol. Phys.* **63**, 527 (1988).
- <sup>21</sup>S. D. Christian and J. F. Scamehorn, in *Surfactant-Based Separation Processes*, edited by F. Scamehorn and J. H. Harwell (Marcel Dekker, New York, 1989), p. 3.
- <sup>22</sup>F. M. Fowkes, *J. Phys. Chem.* **66**, 1863 (1962).
- <sup>23</sup>R. Aveyard, B. P. Brinks, P. Cooper, and P. D. I. Fletcher, *Prog. Colloid Polym. Sci.* **81**, 36 (1990).
- <sup>24</sup>D. J. Mitchell and B. W. Ninham, *J. Chem. Soc., Faraday Trans. 2* **77**, 601 (1981).
- <sup>25</sup>J. Israelachvili, *Intermolecular and Surface Forces*, 2nd ed. (Academic, London, 1991).